Thin Solid Films 569 (2014) 52–56

Contents lists available at ScienceDirect

Thin Solid Films

journal homepage: www.elsevier.com/locate/tsf

Formation of silicon nanocrystal films at low temperature during capacitive radio frequency discharge transition to the high-current mode

Yanmei Xu [a,b], Wei Yu [a,*], Zhaoyi Jiang [a], Yun Li [a], Huimin Li [a], Huina Feng [a]

[a] College of Physics Science and Technology, Hebei University, Baoding, Hebei 071002, PR China
[b] College of Mathematics and Physics, North China Electric Power University, Hebei 071002, PR China

ARTICLE INFO

Article history:
Received 1 June 2013
Received in revised form 25 August 2014
Accepted 28 August 2014
Available online 6 September 2014

Keywords:
Silicon nanocrystal
Crystallinity
Radio frequency discharge
High-current mode

ABSTRACT

In this paper, silicon nanocrystal (Si-nc) films were synthesized via capacitive radio frequency (rf) discharge plasma with silane diluted in helium and hydrogen. The plasma conditions were chosen to simultaneously deposit both Si-ncs and amorphous silicon matrix. The structure and photoluminescence of Si-nc films have been studied. By changing the power delivered to the reactor, the transition from amorphous to crystalline growth in the gas phase can be systematically varied. This transition has been confirmed by detecting the change of current and voltage characteristics of the discharge. The results are interpreted in terms of rf discharge transition to the high-current mode. At high-current mode, plasma density will have a sharp rise by hot electron injection. The high plasma density and hot electrons will increase coupling parameter and cause the transition from amorphous particles to crystal particles.

© 2014 Elsevier B.V. All rights reserved.

1. Introduction

Silicon nanocrystal (Si-nc) films, composed of high-density Si grains separated by the amorphous silicon boundaries, are a material which shows great promise for use in thin-film photovoltaics, because of its higher stability under illumination and high electron mobility, when compared to amorphous silicon films [1–3]. Si-nc films can be grown by solution synthesis, mechanical milling, and particle selection from porous silicon [4,5]. However, it is difficult to control the size uniformity of distributed particles. In vacuum deposition techniques, phase precipitation from Si-rich layer is a common method for crystallizing amorphous Si films in a furnace environment [6,7]. Yet both a high temperature and a long annealing time are necessary. Recent investigations also reported on the gas phase in-situ Si-ncs growth with nonthermal plasmas [8,9], for which high synthesis temperatures can be achieved easily in the gas phase. In this technique uniform and high-density Si-ncs can be produced with nonthermal plasmas. However, the correlation of plasma characteristics with the growth of Si-ncs in the gas phase remains unclear. It is of great technical and scientific interest to understand the formation of Si-ncs.

This paper reports on the deposition experimental studies of Si-ncs embedded in amorphous silicon films. Si-ncs were synthesized in low-pressure nonthermal plasma of hydrogen, helium and silane, which is a typical deposition condition for the powder formation in gas. The formation of Si-nc films in-situ growth is similar but not identical to those known to produce polymorphous silicon films. A main distinction is that Si-ncs formation in the plasma, as opposed to solid-state nucleation of the nanocrystals in the film [10]. Reactive precursor gases are introduced into a chamber where an electrical discharge excites, ionizes and dissociates the gas. Ion-induced nucleation of Si-ncs occurs via clustering of the precursor fragments, and the Si-ncs then grow in size for the duration of their residence in the plasma. Therefore, the characteristic of plasma is important to the formation of Si-ncs. To enhance the crystallization of the particles at room temperatures, we have developed an approach based on capacitive radio frequency (rf) plasma in high-current mode (γ mode). At high discharge, the current ionization is maintained by high-energy electrons initiated at the rf electrodes and the discharge is in the γ mode [11,12]. The plasma characteristics have been investigated in low and high-pressure rf glow discharges [12,13], but it has not been applied in film deposition especially for Si-nc films. In this work, the plasma has been adopted to directly synthesize the films highly packed with Si-ncs. The correlation of the silicon crystallization with the plasma in γ mode will be discussed in detail.

2. Experimental details

Si-ncs were synthesized by rf plasma-enhanced chemical–vapor deposition using a capacitive coupled plasma reactor operated at 13.56 MHz. Fig. 1 shows the schematic drawing of the plasma reactor. The reactor has two parallel round aluminum electrodes with a diameter of 10 mm. The surface of each electrode is covered with square quartz as the dielectric barriers. A gas mixture of helium, silane (5% in helium) and hydrogen was employed as the deposition gas. The gas flow rate of helium, silane (5% in helium) and hydrogen was 30, 5 and 5 sccm, respectively. Several samples were prepared by changing the

* Corresponding author.
E-mail address: ssxym@sohu.com (W. Yu).

http://dx.doi.org/10.1016/j.tsf.2014.08.037
0040-6090/© 2014 Elsevier B.V. All rights reserved.

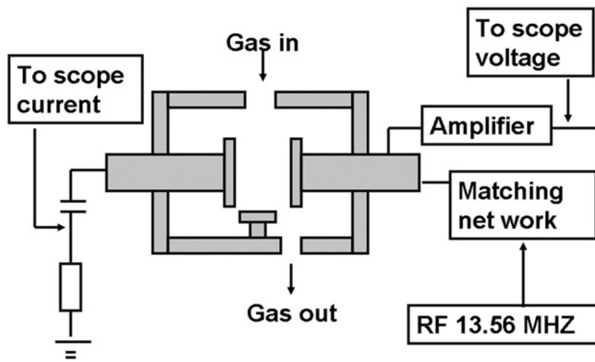

Fig. 1. Schematic of experimental set-up and electrical measurement circuit.

input power while keeping the gas flow rates and chamber pressure constant. The synthesized particles were then drop-cast onto substrates located downstream at the gas outlet of the reaction chamber where Si-nc films formed. The substrate temperature was 200 °C.

The film structure was characterized by X-ray diffraction (XRD, D/max-2400), Transmission Electron Microscopy (TEM, JEOL J2010F(S), operated at 200 keV), and Raman spectroscopy (T 64000 Raman system, with an excitation wavelength of 532 nm). The XRD measurement was carried out with a CuKα target (K = 0.1542 nm) and with a scan rate of 5°/min and a scan rang of 15–70°. The film thickness was measured by the surface profiler (ULVAC, Dektak 3ST). Steady-state photoluminescence (PL) spectra (Edinburgh FLS 920 fluorescence spectrameter) and decay curve of the Si-nc films were done at room temperature. The discharge current through the center element was measured with a shunt resistor. The voltage applied to the top electrode was measured with a 1:1000 high-current probe.

3. Results and discussion

3.1. Structure

Fig. 2 shows the XRD pattern of films deposited at different input powers. The nanoparticles can be obtained as the power ≥60 W, indicated by the diffraction peaks at 28.3°, 47.5°, and 55.9° corresponding to the (111), (220), and (311) planes of silicon, respectively [14,15]. The broad diffraction peak at the low angle originates from the amorphous silicon. The crystallinity increases as the input power increases. As the input power ≤40 W, the samples show mainly amorphous

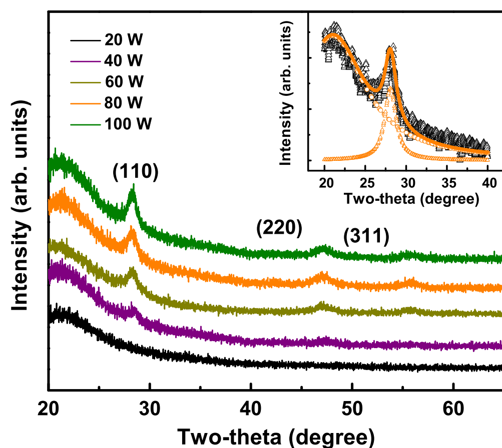

Fig. 2. X-ray diffraction spectra for the samples synthesized at various plasma powers. Peaks corresponding to the (111), (220), and (311) crystallographic planes become visible as the plasma power increases. The inset shows the modeling of the measured section at Si (111).

feature. The average Si crystallite size was estimated to be 3–4 nm using Debye–Scherrer's formula.

Fig. 3 shows the TEM images of samples prepared with input power of 100 W (Fig. 3a) and 20 W (Fig. 3b), respectively. The insets are the corresponding electron diffraction pattern. The TEM images in Fig. 3a confirm the presence of Si-ncs which are embedded in amorphous silicon matrix, with diameters of 3–4 nm. The diffraction pattern (inset in Fig. 3a) also suggests that a large fraction of the particles is crystalline, three rings can be clearly seen, and they can be indexed as the (111), (220), and (311) diffraction rings, respectively. However, in the case of the low-power, there is no sharp bright diffraction ring, apart from a diffuse glow by increasing the contrast ratio (inset in Fig. 3b). That reveals that most of the particles are amorphous silicon and only a small amount of Si-ncs exists in the film [16,17].

The transition from amorphous silicon (a-Si) film to Si-nc film can be observed in Raman spectra, as shown in Fig. 4. As the input power >40 W, silicon crystallite tends to form as indicated by the emerging peak center at around 520 cm^{-1}, which is the Gaussian peak of crystalline silicon. The intensity of this peak increases with increasing input power. In order to evaluate the crystalline volume fraction, the spectra ranging from 400 cm^{-1} to 550 cm^{-1} is deconvoluted into two peaks: one associated to the crystalline Gaussian peaks, I_c (~520 cm^{-1}), and the other is the amorphous Gaussian peak, I_a (~480 cm^{-1}) (see Fig. 4b). The crystalline volume fraction (X_c) is defined as the ratio of the area under the crystalline silicon peak over the sum of the area under the crystalline silicon peak and the area of the amorphous silicon peak, $X_c = I_c/(I_c + \rho I_a)$, where I_c and I_a are the integrated intensities of the amorphous and crystalline peaks, respectively. The ratio of the Raman backscattering cross-section factor ρ is 0.8 which is frequently cited in the literature [18]. The crystalline volume fraction of all samples is plotted as a function of the input power in Fig. 4(b). It is shown that X_c increases monotonically with increasing input power, which is consistent with the above-discussed XRD results.

3.2. Deposition rate

The film deposition rate (R_d) was derived from the film thickness and the deposition time. The deposition rate of the Si-nc films versus the rf power is shown in Fig. 5. Increasing rf power results in the electron density and the density of metastable He atoms in the plasma which promote the dissociation of SiH_4 molecules, leading to higher deposition rate with increasing input power. It should be noted that there is no obvious decrease in deposition rate. In our device, the substrate is perpendicular to the plasma region, which protects the film from the etching process at high rf power.

3.3. Photoluminescence

Fig. 6 shows temperature-dependent PL spectra of as-deposited Si-nc films at high and low input powers. The excitation wavelength is 320 nm. It is observed that the Si-nc films synthesized at 100 W shows a PL peak near 1.6 eV at room temperature. With decreasing temperature the PL intensity of the sample increases by a factor of 1.2 and the PL peak position shifts toward high energy. In Si-nc film, the PL is related to the quantum confinement of Si-ncs, which is weakly dependent on the temperature. The PL peak shifts toward the higher energy region, indicating that the combination of thermal expansion and electron–phonon interaction contributes to an increase of the band gap with decreasing sample temperature [19]. In contrast, the a-Si film synthesized at 20 W shows a PL band near 1.3 eV and the PL intensity is lower than Si-nc film at room temperature. However, at low temperatures, the PL intensity increases by a factor of 40 for a-Si film. This high PL intensity at low temperature is attributed to recombination between electrons trapped in localized conduction–band–tail states and holes trapped in localized valance–band–tail states [20]. The redshift of PL from a-Si

Download English Version:

https://daneshyari.com/en/article/1665252

Download Persian Version:

https://daneshyari.com/article/1665252

Daneshyari.com